Time-varying Hierarchical Archimedean Copulas Using Adaptively Simulated Critical Values

Master Thesis submitted

to

Prof. Dr. Ostap Okhrin

Prof. Dr. Wolfgang K. Härdle

Humboldt-Universität zu Berlin

School of Business and Economics

Institute for Statistics and Econometrics

Ladislaus von Bortkiewicz Chair of Statistics

by

Ramona Theresa Steck

(559948)

in partial fulfillment of the requirements

for the degree of

Master of Science

Berlin, December 09, 2015

Acknowledgement

I would like to express my gratitude to my supervisor, Prof. Dr. Ostap Okhrin, for his support, encouragement and guidance throughout this work. Furthermore I would like to thank my advisor, Prof. Dr. Wolfgang K. Härdle, for his encouragement over the entire course of my studies. I would also like to thank Dr. Andrija Mihoci for all his patience and help.

Abstract

Since recent history has shown that financial crises erupting in one market are likely to spill over to other markets, the analysis of financial contagion attained greater attention. Moreover, there is a common notion among researchers that dependence between financial time series is subject to structural changes. In this paper, financial contagion is modelled by means of hierarchical Archimedean copulas (HAC) for the US, the German and the Japanese stock market. The time-varying nature of the copula parameters is induced by adopting the local parametric approach introduced in Spokoiny (1998) and applied in Härdle et al. (2010). In the latter research paper, the critical values for the sequential testing procedure underlying this approach are simulated on the basis of some predefined copula parameter constellations. However, it is known that the underlying parameter constellations drive the critical values. The contribution of this paper is the adaptive simulation of the critical values according to the "true" parameter constellations. In this way, this paper aims at refining the estimation method conducted in Härdle et al. (2010). It can be seen that the estimation results differ substantially as one simulates the critical values by means of the "true" parameter constellations.

Da in den letzten Jahren deutlich wurde, dass sich Finanzkrisen sehr wahrscheinlich auf anfangs nicht betroffene Märkte ausweiten können, kommt der Analyse des Contagion-Effekts verstärkt Aufmerksamkeit zu. Darüber hinaus stimmen Forscher überein, dass die Abhängigkeit zwischen finanziellen Zeitreihen Strukturbrüchen unterliegt. In dieser Studie wird der Contagion-Effekt zwischen dem US-amerikanischen, dem deutschen und dem japanischen Aktienmarkt mittels hierarchischer Archimedischer Copulas (HAC) untersucht. Um den zeitabhängigen Charakter der Copulaparameter zu berücksichtigen, wird die in Spokoiny (1998) vorgestellte und in Härdle et al. (2010) angewandte Methode übernommen. In Letzterem werden die kritischen Werte der zugrunde liegenden sequentiellen Testprozedur auf Basis vordefinierter Parameterkonstellationen simuliert. Allerdings hängen die kritischen Werte von den wahren Parameterwerten ab. Der Beitrag dieser Studie ist daher die adaptive Simulation der kritischen Werte anhand der "wahren" Parameterkonstellationen. Es fällt auf, dass sich die Schätzergebnisse mit adaptiv simulierten kritischen Werten erheblich von den Ergebnissen mit vorab simulierten kritischen Werten unterscheiden.

Keywords: Hierarchical Archimedean copula, local parametric approach, sequential testing procedure, interval of homogeneity, adaptive simulation, critical values.

Contents

List of Abbreviations

AC	Archimedean copula(s)	BIC	Bayesian information criterion
BL	Box-Ljung test	DJ	Dow Jones
HAC	Hierarchical Archimedean copula(s)	KS	Kolmogorov-Smirnov test
LCP	Local Change Point	ML	Maximum likelihood
SMB	Small modelling bias		

List of Figures

List of Tables

1 Introduction

Globalisation and especially the reduction of trade restrictions have led to the fact that financial markets have become more and more integrated in the course of the last years. These increasing interrelations, however, entail a serious risk of financial contagion as has already been experienced in recent history. One frequently cited example is the Asian financial crisis which erupted in Thailand in 1997. Soon after the outbreak of the crisis, it affected neighbouring countries such as Indonesia or South Korea and eventually had an impact on Latin America. The global financial crisis of 2007-2009 serves as another good example of the disadvantages of tightly interconnected markets. Having emerged in the US subprime mortgage market, it rapidly spilled over to developed and emerging countries, some of which suffered from even stronger stock market crashes than the US (Bergmann et al., 2015). As a consequence, a lot of research has lately been devoted to the phenomenon of financial contagion and its evolution over time.

In order to examine financial contagion, the degree of interdependence between financial markets has to be analysed. The standard and most widely used statistical tool for modelling dependence is Pearson's correlation coefficient. Applying it to financial data, however, is highly questionable. Researchers have agreed on the notion that log returns of stock prices follow heavy-tailed and possibly skewed distributions. Thus, allowing for infinite variances, the correlation coefficient might not be defined, and in case of non-elliptical distributions a zero correlation coefficient does not indicate independence between stock returns. Furthermore, the correlation is not invariant to nonlinear strictly increasing transformations of random variables. This turns out to be a serious problem when dealing with log returns since stock prices are related to them in a nonlinear and strictly increasing way. These limitations of Pearson's correlation coefficient are mentioned in Rachev et al. (2005). An alternative approach, which remedies these drawbacks, is to study dependence using copulas which are first introduced in Sklar (1959). However, the ideas underlying the concept of copulas date back to Hoeffding (1940). A copula specifies the functional link between the marginal distributions and the joint distribution of random variables. It clearly characterizes the structure of dependence and gives the opportunity to describe the coherence between tail events of distributions. Hence, copulas are well-suited for the analysis of dependence between stock returns.

Financial time series and, therefore, the dependence structure between them are subject to

structural breaks caused by regime or market changes. Evidence for the time variation of the dependence between financial time series can be found in Patton (2006). In this research paper, time-varying copulas are applied to study asymmetries in the dependence structure of exchange rates. As reported in Rodriguez (2007), a change in the dependence structure between stock indices occurs at times of financial turbulences. Within the scope of this study, copulas with Markov switching parameters are applied to East Asian stock indices during the period of the Asian crisis. The main statement of this work is that structural changes in tail dependence are an essential circumstance that must not be neglected when studying financial contagion. Giacomini et al. (2006) concerns the application of a novel estimation method that allows for adaptively estimated time-varying parameters of copulas and builds on the local parametric approach suggested in Spokoiny (1998). The main assumption is that there exists a homogeneous interval in a time series where the copula parameters can be well described by constants. In Härdle et al. (2010), structural breaks in the dependence between financial time series are allowed by applying the same adaptive estimation approach. In order to model coherence of stock indices and exchange rates, they estimate hierarchical Archimedean copulas (HAC) with time-varying parameters. Since HAC are comprised of dependence parameters and a structure parameter, the researcher can observe whether a change in dependence is merely due to a change in the strength or also to a change in the form of the dependence (Härdle et al., 2010).

In the present empirical study, the same adaptive estimation procedure as in Giacomini et al. (2006) and Härdle et al. (2010) is employed to investigate the time variation of the parameters of HAC for the Japanese, the German and the US stock market. At each point in time, the estimation method demands a test of local homogeneity against a change point alternative on several intervals of ascending lengths. In Härdle et al. (2010), the critical values for this sequential testing procedure are simulated on the basis of some pre-specified parameter constellations. However, the critical values depend on the true parameter values underlying the respective interval. The contribution of this paper is therefore a refinement of the computation of the critical values used for the completion of the estimation approach. They are obtained in a more data-driven way. In Härdle et al. (2012), the parameter constellations for the simulations are selected by means of estimates obtained from a rolling window estimation of the time series. By contrast, the present research work builds on critical values that are simulated based on the "true" parameters that are estimated at the point in time and on the interval under consideration. First of all, the local parametric approach is carried out using

the critical values obtained as in Härdle et al. (2010). Then, the procedure is conducted a second time, but on the basis of the refined critical values. To conclude, the results of the two different approaches are investigated thoroughly and compared.

The remainder is structured as follows. The coming section gives a brief introduction to the concept and estimation of HAC. The local parametric approach proposed in Spokoiny (1998) is discussed in Section 3. The data used for the empirical analysis are presented in Section 4. Section 5 concerns the application of the local parametric approach to the data and the discussion of the results. Conclusions are drawn in Section 6.

2 Hierarchical Archimedean Copulas

As stated in Sklar (1959), a unique copula specified as a continuous function $C : [0,1]^d \to [0,1]$ exists if F is an arbitrary d-dimensional joint distribution function with continuous margins $F_1, ..., F_d$. A copula satisfies the following equality:

$$C(u_1, ..., u_d) = F\{F_1^{-1}(u_1), ..., F_d^{-1}(u_d)\}, \qquad u_1, ..., u_d \in [0,1]. \tag{1}$$

$F_1^{-1}(u_1), ..., F_d^{-1}(u_d)$ denote the quantile functions of the associated marginal distributions $F_1(x_1), ..., F_d(x_d)$. There are different families of copulas. On the one hand, there are elliptical copulas such as the Gaussian copula. These copulas, however, suffer from the fact that they do not exhibit closed form expressions. Moreover, they are confined to modelling symmetric dependence among variables. Thus, this class of copulas cannot account for the typical feature of dependence in financial markets, namely asymmetry. These drawbacks are mentioned for example in Embrechts et al. (2001). On the other hand, there is the family of Archimedean copulas which is dealt with for instance in Genest and MacKay (1986), Joe (1997) and Nelsen (1999). These copulas are not inferred from multivariate distribution functions, but can be given explicitly with the help of generator functions satisfying several conditions. However, Archimedean copulas have certain disadvantages which are discussed for example in Härdle et al. (2010). They are referred to as being "exchangeable" meaning that the dependence is the same although the variables are permuted. Furthermore, they are rather restrictive since they characterize the dependence structure solely by one single parameter. In order to overcome these limitations, a generalization of the Archimedean copula is presented in Joe (1997). It is referred to as a fully nested hierarchical Archimedean copula (HAC). The

formula is given in Härdle et al. (2010) by

$$C(u_1,...,u_d) = C_1\{C_2(u_1,...,u_{d-1}),u_d\} = \phi_1\{\phi_1^{-1}\circ C_2(u_1,...,u_{d-1}) + \phi_1^{-1}(u_d)\}$$
$$= \phi_1\{\phi_1^{-1}\circ\phi_2(\phi_2^{-1}(C_3(u_1,...,u_{d-2})) + \phi_2^{-1}(u_{d-1})) + \phi_1^{-1}(u_d)\}. \quad (2)$$

The function $\phi : [0,\infty) \to [0,1]$ is called copula generator and ϕ^{-1} is its pseudo-inverse given by $\phi^{-1}(u) = inf\{t : \phi(t) \leq u\}$. Two well known copula generators are the Gumbel generator defined as $\phi = exp(-t^{1/\theta})$ with $\theta \in [1,\infty)$ and the Clayton generator given by $\phi = (1+t)^{-1/\theta}$ with $\theta \in (0,\infty)$ (Joe, 1997). A copula generator ϕ is a continuous, decreasing and convex function with $\phi(0) = 1$ and $\phi(\infty) = 0$. In addition, ϕ is required to be completely monotonic fulfilling $(-1)^j\phi^{(j)}(x) \geq 0$ for all $j \geq 0$. For reviews of the conditions of the copula generator see Kimberling (1974) and McNeil (2008). These conditions must also hold in the exchangeable case of Archimedean copulas. However, for the special case of fully nested HAC (2), a further requirement has to apply. If ϕ_i for $i = 1,...,d-1$ are generator functions satisfying the above mentioned conditions, and $\phi_i^{-1}\circ\phi_{i+1}$ have completely monotonic derivatives for $i = 1,...,d-2$, then $C(u_1,...,u_d)$ from (2) is a copula (McNeil, 2008). For a more descriptive representation of HAC, consider the following special case of fully nested HAC with $d = 3$:

$$C(u_1,u_2,u_3;s,\theta_1,\theta_2) = C_1\{C_2(u_1,u_2;\theta_1),u_3;\theta_2\}$$
$$= \phi_{1,\theta_2}\{\phi_{1,\theta_2}^{-1}\circ C_2(u_1,u_2;\theta_1) + \phi_{1,\theta_2}^{-1}(u_3)\}$$
$$= \phi_{1,\theta_2}\{\phi_{1,\theta_2}^{-1}\circ(\phi_{2,\theta_1}\{\phi_{2,\theta_1}^{-1}(u_1) + \phi_{2,\theta_1}^{-1}(u_2)\} + \phi_{1,\theta_2}^{-1}(u_3)\}. \quad (3)$$

Note that this representation includes the copula parameters s,θ_1 and θ_2. The parameter s stands for the structure of the HAC. In this case, $s = ((1.2).3)$ since the variables u_1 and u_2 are coupled together first in copula C_2. The strength of the dependence between u_1 and u_2 is given by the parameter θ_1 of the copula generator ϕ_2. The parameter θ_2 measures the dependence between the remaining variable u_3 and the copula C_2, which is treated as a new variable. θ_2 is the parameter referring to the copula generator ϕ_1. In the following, s is referred to as the structure parameter and θ_1 and θ_2 as the dependence parameters of the HAC. A similar formulation of (3) extended to the d-dimensional case can be found in Härdle et al. (2010). In this study, the generators ϕ_i within a HAC are restricted to the same generator family, i.e. when ϕ_2 in (3) is a Gumbel generator, so is ϕ_1. As addressed in Härdle et al. (2010), the required complete monotonicity of coupled generators in a HAC enforces some restrictions on the dependence parameters in such cases. For most copula generators, a descent in the parameter values from the first stage to higher stages of a HAC is postulated.

This means that in (3) the inequality $\theta_1 > \theta_2$ has to be fulfilled.

While exchangeable Archimedean copulas are characterized merely by one parameter, the HAC in (3) depends on three copula parameters, namely s, θ_1 and θ_2. On the one hand, this fact makes HAC more flexible, whereas on the other hand it exacerbates the estimation process. An efficient recursive way of estimating the parameters of HAC is proposed in Okhrin et al. (2013) and also applied in Härdle et al. (2010). In the first step, a bivariate copula is fitted to all possible combinations of the variables. For example, in (3) with $d = 3$ there are three different combinations which are $(u_1, u_2), (u_1, u_3)$ and (u_2, u_3). The pair of variables with the strongest dependence is chosen and the estimated parameter of the first step is denoted by $\hat{\theta}_1$. This pair of variables is then coupled to build the new pseudo-variable $C\{\hat{\theta}_1, \phi_1\}$. In (3) this pseudo-variable corresponds to C_2. In the next step, all possible pairs of the remaining variables and the new pseudo-variable are considered and all previous sub-steps repeated. To sum up, the dependence parameter at a certain stage is estimated taking the dependence parameters and marginal distributions at lower stages of the estimation process for granted. In the present paper, the dependence parameters on the bivariate copula level are estimated nonparametrically using Kendall's τ. Kendall's τ measures the difference between the probability of getting a concordant pair and the probability of getting a disconcordant pair of observations of random variables. The population version of Kendall's τ is given by

$$\tau = \Pr((X_i - X_j)(Y_i - Y_j) > 0) - \Pr((X_i - X_j)(Y_i - Y_j) < 0), \tag{4}$$

where (X_i, Y_i) and (X_j, Y_j) are a pair of independent random vectors of the variables (X, Y). This formula is presented in and Embrechts et al. (2001) and Górecki and Holeňa (2013). To eventually obtain the copula parameter θ, the relationship $\theta = \frac{1}{1-\tau}$ provided in Embrechts et al. (2001) is employed in the case of a Gumbel generator. In addition, the range of permissible values of Kendall's τ amounts to $[0, 1)$. This estimation approach is briefly mentioned in Okhrin et al. (2013).

3 Local Parametric Modelling

It is a common notion that financial time series are subject to structural breaks induced by regime or market changes. The same is also true for the dependence between financial time series. Evidence supporting this proposition can be found in Patton (2006) and Rodriguez (2007). In order to obtain consistent parameter estimates, structural breaks altering a time

series model should not be neglected. For the analysis of consequences of ignored structural breaks refer to Andreou and Ghysels (2008). In the present empirical study, a local parametric approach first suggested in Spokoiny (1998) is employed. This modelling approach allows for time-varying parameters such that structural breaks are automatically taken into consideration. The core idea of this approach is that there exists a homogeneous interval in a time series on which the model parameters can be appropriately measured by constants. Theory and applications of the local parametric approach are presented for example in Mercurio and Spokoiny (2004), Čížek et al. (2009) and Härdle et al. (2010).

3.1 Statistical Framework

The main goal of the local parametric approach is to detect the interval I which is closest to the so-called "oracle" interval. The "oracle" interval I_{k^*} is defined as the longest interval $I = [t_0 - m_{k^*}; t_0]$, for which the following condition taken from Härdle et al. (2010) holds:

$$\Delta_I(s, \theta) = \sum_{t \in I} \mathcal{K}\{C(\cdot; s_t, \theta_t), C(\cdot; s, \theta)\} \leq \Delta, \tag{5}$$

for some $\Delta \geq 0, s, \theta$. Condition (5) is designated as small modelling bias (SMB) condition (Härdle et al., 2010). An important ingredient in (5) is the Kullback-Leibler divergence $\mathcal{K}$ which gives the disparity of the copulas $C(\cdot; s, \theta)$ and $C(\cdot, s_t, \theta_t)$:

$$\mathcal{K}\{C(\cdot; s_t, \theta_t), C(\cdot; s, \theta)\} = \mathbb{E}_{s_t, \theta_t} \log \frac{c(\cdot; s_t, \theta_t)}{c(\cdot; s, \theta)}. \tag{6}$$

$c(\cdot)$ stands for the copula density. s_t and θ_t are the unknown time-varying copula parameters, whereas s and θ are locally constant parameters which can be estimated on interval I for the point in time t_0. The optimal estimates for s and θ can be obtained on the largest interval $\text{argmax}_I \Delta_I(s, \theta) = [t_0 - m_{k^*}; t_0]$ for which the SMB condition (5) is valid. These estimates then constitute adequate approximations for the latent time-varying parameters. The aforementioned theoretical aspects are presented in Härdle et al. (2010). In summary, the local parametric approach intends to maintain an appropriate trade-off between estimation precision and modelling bias (Härdle et al., 2012).

3.2 Local Change Point (LCP) Detection

As mentioned above, the true time-dependent copula parameters s_t and θ_t are unknown such that the "oracle" interval cannot be identified either. Therefore, a sequential testing

procedure known as Local Change Point (LCP) Detection, see Spokoiny (2009), is employed. The aim is to detect best possible intervals characterized by parameter homogeneity. For a

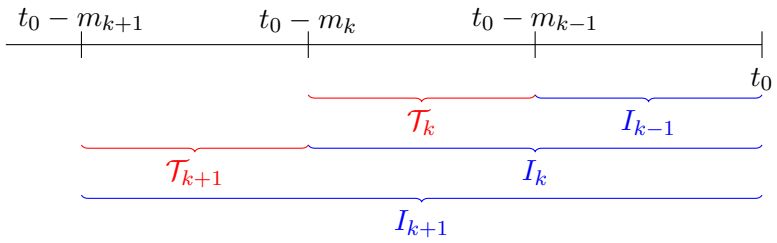

Figure 1: Interval selection.

better understanding of the sequential testing procedure, have a look at Figure 1. Consider a sequence of interlaced interval candidates $I_k \subset I_{k+1}$ with the same end point t_0 on the right. In the first step, one tests whether a change point has occurred in $\mathcal{T}_k = I_k \setminus I_{k-1}$ assuming parameter homogeneity within I_{k-1}. If a change point cannot be found within $\mathcal{T}_k$, parameter homogeneity is accepted for interval I_k. The following step is then to decide about the next larger interval I_{k+1} by checking the subset $\mathcal{T}_{k+1} = I_{k+1} \setminus I_k$ for a change point. The algorithm stops as soon as the largest possible interval has been reached or a change point has been detected at an earlier stage. In the latter case, one sticks with the last interval for which parameter homogeneity was not rejected. For instance, if a change point was detected within interval I_{k+1}, the next shorter interval I_k would be used for the estimation of the copula parameters at time point t_0. The interval candidates for the testing procedure have to be set by the researcher in advance. In this research work, the interval candidates are selected in terms of a geometric grid as in Härdle et al. (2010) and Härdle et al. (2012). The length of the shortest interval I_0 is set to m_0. The lengths of the subsequent intervals evolve via the formula $m_k = [m_0 c^k]$ for $k = 1, 2, ..., K$ and $c > 1$. $[x]$ stands for the integer part of x. In the present study, the sequence of intervals is defined by $m_0 = 40,\ c = 1.25$ and $k = 1, ..., 10$. Hence, the interval lengths are $I_1 = 50,\ I_2 = 62, ..., I_{10} = 372$.

The hypotheses for the local change point test on interval I_k can be formulated as:

$$H_0 : \ \forall \tau \in \mathcal{T}_k, \theta_t = \theta, s_t = s, \forall t \in I_{k+1} = J \cup J^C = [\tau, t_0] \cup [t_0 - m_{k+1}, \tau) \tag{7}$$

$$H_1 : \ \exists \tau \in \mathcal{T}_k, \theta_t = \theta_1, s_t = s_1, \forall t \in J = [\tau, t_0]$$
$$\text{and } \theta_t = \theta_2 \neq \theta_1 \text{ or } s_t = s_2 \neq s_1, \forall t \in J^C = [t_0 - m_{k+1}, \tau). \tag{8}$$

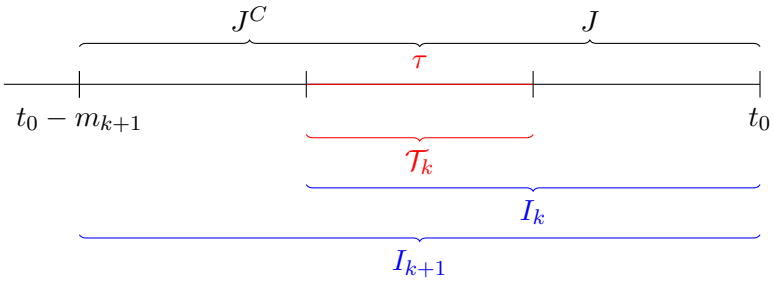

Figure 2: Relevant intervals for the test statistic.

In other words, under H_0 the observations in I_k correspond to a model with constant parameters s and θ. The alternative hypothesis states that at least one of the parameters s and θ was subject to significant changes at some location τ within interval I_k. A very similar formulation of the hypotheses can be found in Giacomini et al. (2006) and Härdle et al. (2010). The respective likelihood ratio test for a change point at fixed location τ within interval I_k can be written as:

$$\begin{aligned} T_{I_k,\tau} &= \max_{s_1,\theta_1,s_2,\theta_2} \{\ell_J(s_1,\theta_1) + \ell_{J^C}(s_2,\theta_2)\} - \max_{s,\theta} \ell_{I_{k+1}}(s,\theta) \\ &= \ell_J(\hat{s}_1,\hat{\theta}_1) + \ell_{J^C}(\hat{s}_2,\hat{\theta}_2) - \ell_{I_{k+1}}(\hat{s},\hat{\theta}). \end{aligned} \tag{9}$$

The likelihood function $\ell_{I_{k+1}}(s,\theta)$ corresponds to the model under H_0, whereas the likelihood function $\ell_J(s_1,\theta_1) + \ell_{J^C}(s_2,\theta_2)$ relates to H_1. ℓ_I denotes the likelihood function for interval I. For a graphical illustration of the intervals involved in the implementation of the test, regard Figure 2. Since the exact location of τ is unobserved, the test statistic is defined as:

$$T_{I_k} = \max_{\tau \in \mathcal{T}_k} T_{I_k,\tau}. \tag{10}$$

The test decision is based on a comparison of the test statistic T_{I_k} with the critical value ξ_k in the sense that the null hypothesis of parameter homogeneity is rejected for interval I_k if $T_{I_k} > \xi_k$. Since the critical values for the testing procedure depend on several parameters including the interval lengths and the dependence parameters, their calculation is demanding. Therefore, they are discussed separately in the next subsection.

3.3 Critical Values

In this empirical study, the critical values are calculated in two different ways. First of all, they are calculated in the same way as in Härdle et al. (2010). However, following this approach, the critical values do not correspond to the true underlying copula parameters.

Therefore, an alternative way for computing the critical values, which aims at refining the first mentioned approach, is introduced as well. Both approaches build on the sequential choice of critical values ξ_k presented in Spokoiny (2009).

If the null hypothesis of parameter homogeneity holds, the largest interval I_K of those taken into consideration is the ideal choice for the estimation of the copula parameters at time point t_0. A so-called "false" alarm occurs when the procedure selects a shorter interval I_k for $k < K$ such that the adaptive estimator does not refer to the largest permitted interval. By applying the sequential choice proposed in Spokoiny (2009), the critical values are chosen to minimize the probability of this false alarm. This means that the critical values are selected such that the condition

$$\mathbb{E}_{s^*,\theta^*}|\ell(\tilde{s}_k,\tilde{\theta}_k) - \ell(\hat{s}_k,\hat{\theta}_k)|^r \leq \rho\frac{k}{K}\mathcal{R}_r(s^*,\theta^*) \tag{11}$$

is maintained. $\mathcal{R}_r(s^*,\theta^*) = \max_k |\ell(\tilde{s}_k,\tilde{\theta}_k) - \ell(s^*,\theta^*)|^r$ is the parametric riskbound which constrains the log-likelihood loss arising from the estimation of the true parameters (s^*,θ^*) by the estimates $(\tilde{s}_k,\tilde{\theta}_k)$ from the ideal interval choice. Condition (11) guarantees that the loss relating to a false alarm represented by the estimates $(\hat{s}_k,\hat{\theta}_k)$ does not exceed a ρ-fraction of the loss caused by the ideal estimate $(\tilde{s}_k,\tilde{\theta}_k)$. The parameter r denoting the power of the loss in (11) is set to 0.5 throughout the empirical study. The parameter ρ can be interpreted in a similar way as the significance level and is fixed at 0.5. ρ drives the sensitivity of the testing procedure to inhomogeneity in the sense that an increase of it leads to smaller critical values. The aforementioned theoretical aspects are also discussed in Čížek et al. (2009) and Härdle et al. (2010).

Consider the following: The situation after k steps can be twofold. Either a change point is found at some step $l \leq k$ or no change point is identified at all. Adhering to the notation in Spokoiny (2009), the event B_l referring to the rejection of the null hypothesis in step l corresponds to:

$$B_l = \{T_1 \leq \xi_1, ..., T_{l-1} \leq \xi_{l-1}, T_l > \xi_l\}. \tag{12}$$

In such a case, the estimated copula parameters of step k denoted as $(\hat{s}_k,\hat{\theta}_k)$ conform to the estimates obtained on the previous accepted interval, which are given by $(\tilde{s}_{l-1},\tilde{\theta}_{l-1})$, for $l = 1, ..., k$. By means of Monte-Carlo simulations, the critical value ξ_l is determined

adaptively as the minimal value that fulfils the inequality below:

$$\max_{k=l,...,K} E_{s^*,\theta^*}|\ell(\tilde{s}_k, \tilde{\theta}_k) - \ell(\tilde{s}_{l-1}, \tilde{\theta}_{l-1})|^r \mathbf{I}(B_l) \leq \rho \frac{k}{K} \mathcal{R}_r(s^*, \theta^*). \tag{13}$$

I in (13) stands for the indicator function. When $l = 1$, the above inequality depends solely on the first critical value denoted by ξ_1. In every subsequent step $l \geq 2$, the critical values $\xi_1, ..., \xi_{l-1}$ are treated as given from the preceding steps. Thus, the event B_l is driven merely by the critical value ξ_l. The programming work for the calculation of the critical values is strongly oriented to the proposal given in Neubauer (2012).

3.3.1 First Approach

The first approach to calculating the critical values corresponds to the one conducted in Härdle et al. (2010). The simulations are carried out according to Algorithm 1 in Okhrin and Ristig (2014) which is proposed in Hofert and Maechler (2011). The model under consideration is a three-dimensional HAC only comprised of Gumbel generators. In order to simulate from the HAC, the copula parameters are set by the researcher. While a definition of the structure parameter s is not necessary, the dependence parameters θ_1 and θ_2 are essential ingredients in the calculation of the critical values. The parameter constellations are chosen as $\theta = (\theta_1, \theta_2)^\top = \{\theta(\tau_1), \theta(\tau_2)\}^\top$ where $\{\tau_1, \tau_2\} \in \{0.1, 0.3, 0.5, 0.7\}^2,\ \tau_1 \geq \tau_2$. Making use of the relationship between Kendall's τ and the Gumbel copula parameter θ, this translates into $\{\theta_1, \theta_2\} \in \{1.11, 1.43, 2, 3.33\}^2,\ \theta_1 \geq \theta_2$. Note that this yields ten different parameter combinations and therefore ten curves of critical values. In the case of $\theta_1 = \theta_2$, the simulations are run based on an exchangeable three-dimensional Archimedean copula $C(u_1, u_2, u_3; \theta)$ which is characterized merely by one parameter, namely $\theta = \theta_1 = \theta_2$. In all other cases, one simulates from a HAC given by $C\{u_1, C(u_2, u_3; \theta_1); \theta_2\}$. For the simulation of the critical values ξ_k, $N = 10,000$ samples of size $n = [m_0 c^{K+1}] + 1$ are generated exploiting the above mentioned geometric grid of the intervals, $k = 1, 2, ..., K = 10$. Recall from Section 3.2 that the critical values depend on the interval lengths and the dependence parameters. Figure 3 depicts the critical values obtained for different values of τ_1 as a function of k. It clearly demonstrates that the larger the interval (indicated by a higher k), the smaller is the critical value. This is related to the fact that for smaller k the parameter estimator is more volatile. In addition, it is obvious from Figure 3 that higher values of the dependence parameters (here: τ_1) tend to result in higher critical values holding k constant. Due to these influences, the critical value for a certain point in time t_0 and interval length m_k has to be selected appropriately from the ones available through the simulations. This is done in the following way: At each point

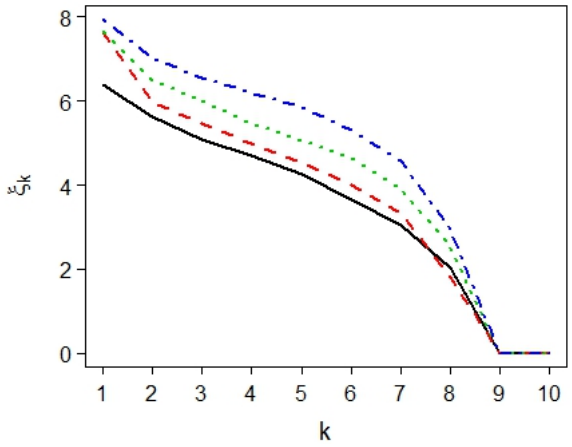

Figure 3: Simulated critical values as a function of k for fixed $\tau_2 = 0.1$ with $\tau_1 = 0.1$ (black), $\tau_1 = 0.3$ (red), $\tau_1 = 0.5$ (green), $\tau_1 = 0.7$ (blue).

in time t_0 a local HAC is estimated on a given interval. The corresponding critical value is then chosen according to the length of the interval and the parameter constellations that are closest to the estimates from the local HAC. In this manner, the selected critical value does not fully reflect the true underlying parameter constellations. As a consequence, one has to hazard a certain degree of inaccuracy of the adaptive estimator. The main reason for this is that one can hardly consider an unlimited number of predefined parameter constellations for the simulations. The dependence parameters, however, can take on infinitely many values. To overcome this drawback, a second approach to obtaining the critical values is introduced in the next section. It intends to yield a refinement of the above illustrated approach. In the subsequent sections, the first approach which resembles the one implemented in Härdle et al. (2010) is referred to as pre-simulation approach.

3.3.2 Second Approach

The second approach differs from the previous one in that it determines the critical values in a completely data-driven way. Instead of using predefined parameter constellations, it relies exactly on the parameter estimates that are obtained during the implementation of the sequential testing procedure. The approach can be described as follows: Consider interval I_k shown in Figure 4 as a candidate for the estimation of the HAC at time point t_0. As before, a local HAC is estimated on the given interval. Denote the estimated HAC by $\hat{C}^* = C(\hat{s}^*, \hat{\theta}^*)$. In place of selecting the critical value according to the closest parameter

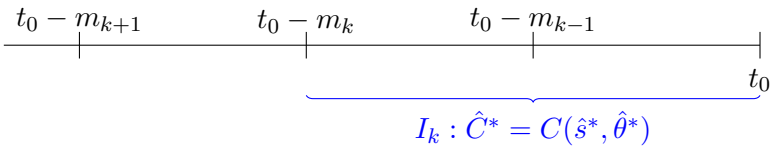

Figure 4: Estimated copula for simulations of critical values.

constellation, simulations are now carried out directly from the estimated HAC $\hat{C}^*$. The simulations are performed as before according to Algorithm 1 from Okhrin and Ristig (2014) with the sole difference that the number of samples is set to $N = 1,000$. In the next step, the riskbound $\mathcal{R}_r(s^*, \theta^*)$ is calculated with $(s^*, \theta^*) = (\hat{s}^*, \hat{\theta}^*)$. This means that the estimated parameters $(\hat{s}^*, \hat{\theta}^*)$ from interval I_k represent the "true" parameters. The corresponding critical value is then obtained from a slightly modified condition (13) given by

$$\max_{k=l,...,K} E_{\hat{s}^*,\hat{\theta}^*} |\ell(\tilde{s}_k, \tilde{\theta}_k) - \ell(\tilde{s}_{l-1}, \tilde{\theta}_{l-1})|^r \mathbf{I}(B_l) \leq \rho \frac{k}{K} \mathcal{R}_r(\hat{s}^*, \hat{\theta}^*). \tag{14}$$

In line with the pre-simulation approach, B_l defined in (12) is controlled merely by the critical value ξ_l. All other critical values $\xi_1, ..., \xi_{l-1}$ are known from previous calculation steps at t_0. Now, the critical value ξ_l is valid only for the given interval I_k and the associated time point t_0. It is then compared to the respective test statistic. If the null hypothesis of parameter homogeneity is rejected, the testing procedure is done with the selection of an interval for the HAC at t_0. In such an event, the critical values $\xi_{l+1}, ..., \xi_K$ corresponding to the steps not yet taken into account are not calculated. If the null hypothesis is not rejected, the procedure jumps to the next larger interval I_{k+1}. The same steps are taken as for interval I_k. This particularly means, that simulations have to be rerun, but this time from the HAC $\hat{C}^*$ estimated on I_{k+1}. Hence, curves of critical values each referring to one certain parametric model as in the preceding section are no longer obtained. Now, each individual critical value originates from one specific parametric model. In the coming sections, this approach is referred to as the second approach or adaptive simulation approach.

4 Data

The dataset that is used for the empirical analysis contains three major stock indices each representing one leading stock market. The considered indices are DAX, Dow Jones (DJ) and Nikkei as in Härdle et al. (2010). The regarded time period, however, distinguishes the datasets. In the present study, the data range from 01.06.2005 to 29.05.2015 taking recent political and economic incidents into account. This yields 2608 observations per index. The data are provided by Datastream. Before beginning with the analysis, the daily log returns of the stock indices are computed. They are later used throughout the study. The performance of the indices and the corresponding return series are displayed in Figure 5.

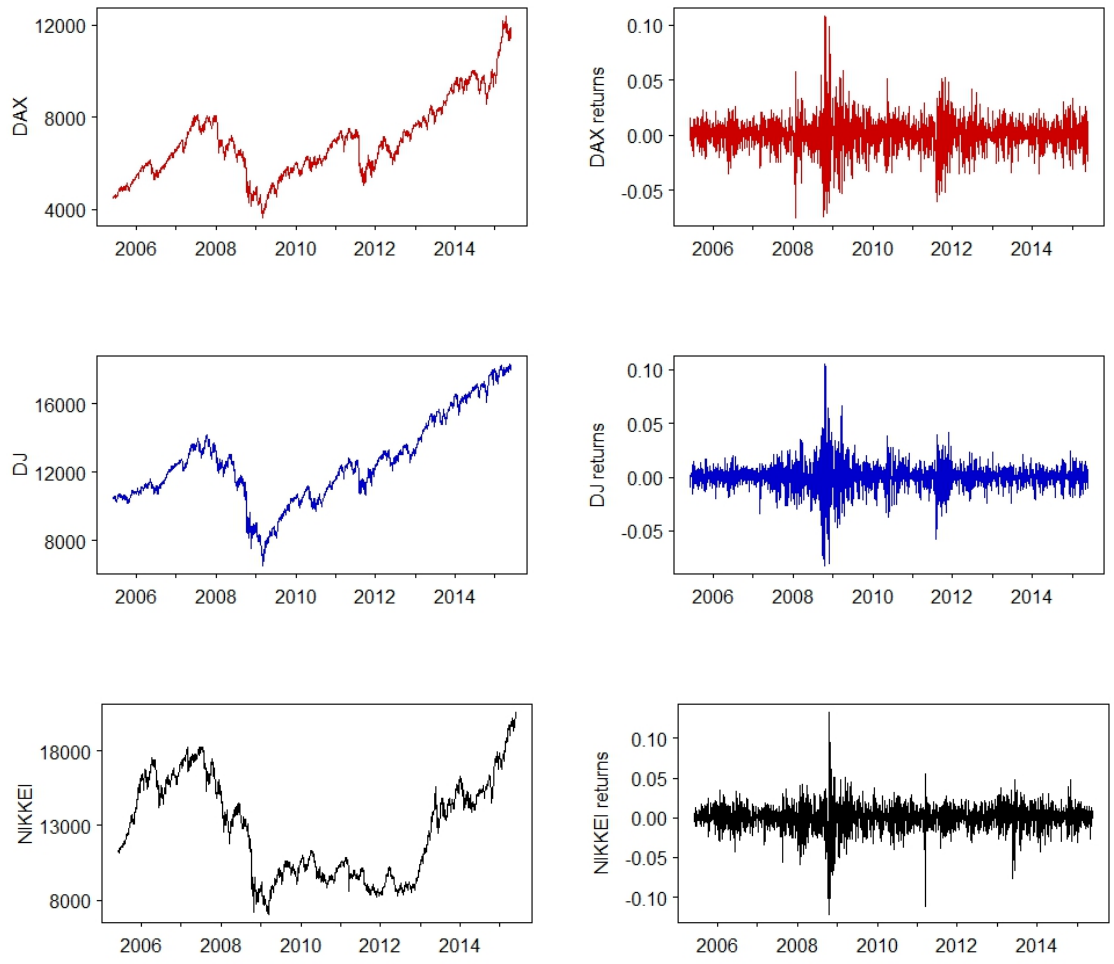

Figure 5: Index values and log returns for DAX, Dow Jones (DJ) and Nikkei across time.

It is striking that all three indices drop sharply around 2009 when the global financial crisis was in full swing. The returns exhibit increased volatility at the same time. The performances of DAX and Dow Jones are quite similar, whereas the performance of Nikkei differs more. The coming section provides a deeper insight into the dependencies between the returns of the considered stock indices.

5 Empirical Study

This section focuses on the implementation of the empirical analysis and the discussion of the acquired results. It is structured as follows: First, the log returns of DAX, Dow Jones and Nikkei undergo little preprocessing. Second, the application of the sequential testing procedure is motivated on the basis of the data at hand. Third, the sequential testing procedure is carried out. The first run of the procedure relies on the critical values obtained in the pre-simulation approach presented in Section 3.3.1. The second run uses adaptively simulated critical values as discussed in Section 3.3.2. The results from both approaches are then described and compared.

5.1 Preprocessing

As observed in Mandelbrot (1963), large changes in a time series are rather followed by further large changes, and so are small changes by other small changes. This phenomenon is known as volatility clustering. It is also manifested by a positive slowly decaying autocorrelation function for absolute or squared returns when returns themselves do not exhibit any autocorrelation (Cont, 2005). The returns are uncorrelated in such cases, but clearly not independent. Volatility clustering is usually present in financial time series. Having a look at the return series of the indices shown in Figure 5, one notices that the period before 2008 is characterized by a low degree of volatility. Starting around 2008, however, volatility has increased for a certain length of time. This is particularly remarkable for DAX and Dow Jones. In order to get rid of volatility clusters in the present data, a univariate GARCH(1,1) model is fitted to each of the return series. The model is given by

$$X_t = \mu_t + \sigma_t \epsilon_t \text{ with } \sigma_t^2 = \omega + \alpha \sigma_{t-1}^2 \epsilon_{t-1}^2 + \beta \sigma_{t-1}^2 \tag{15}$$

where $\omega > 0,\ \alpha \geq 0,\ \beta \geq 0$ and $\alpha + \beta < 1$. The GARCH model is introduced in Bollerslev (1986). The errors are assumed to follow a skewed Student's t-distribution. This distribution is chosen due to its property of modelling asymmetry in data. It additionally requires the

	$\hat{\mu}_j$	$\hat{\omega}_j$	$\hat{\alpha}_j$	$\hat{\beta}_j$	$\hat{\gamma}_j$	$\hat{\nu}_j$	BL	KS
DAX	0.001	2.272e-06	0.098	0.894	0.925	6.451	0.965	1.938e-05
	(0.0002)	(7.153e-07)	(0.014)	(0.014)	(0.023)	(0.916)		
DJ	0.001	1.382e-06	0.112	0.881	0.926	5.320	0.221	9.064e-08
	(0.0001)	(3.944e-07)	(0.016)	(0.015)	(0.023)	(0.653)		
NIKKEI	0.001	3.577e-06	0.093	0.892	0.925	8.138	0.900	3.082e-06
	(0.0002)	(1.039e-06)	(0.013)	(0.014)	(0.024)	(1.380)		

Table 1: Estimated parameters and p-values from fitting GARCH(1,1). The corresponding standard deviations are provided in parentheses. The last two columns show the p-values of the Box-Ljung test (BL) for 12 lags and the Kolmogorov-Smirnov test (KS) for the studentized residuals.

estimation of a skew parameter and a shape parameter denoted as γ and ν, respectively. The residuals from fitting the GARCH(1,1) model are studentized. The results of the estimation are summarized in Table 1. Note that all estimated parameters are statistically significant. The Box-Ljung test (BL) proves the null hypothesis of no autocorrelation in the residuals. In the present study, 12 lags are included in the test. For none of the indices the residuals exhibit a significant autocorrelation. The Kolmogorov-Smirnov test (KS) is based on a comparison between the empirical distribution function of a sample and a theoretical cumulative distribution function. Considering the normal distribution as the theoretical one, the null hypothesis states that the residuals are normally distributed. The p-values for the KS show that the null hypothesis is rejected in all three cases. The fact that the residuals are not normal suggests that the margins for the copula model should be estimated in a nonparametric way. The following analysis refers exclusively to the series of residuals as they are adjusted for volatility clusters.

5.2 Rolling Window Estimation

In order to get a first idea of the time variation of the dependencies between the GARCH(1,1) residuals, consider Figure 6. Following Härdle et al. (2010), it shows the evolution of two measures of association, namely Pearson's correlation coefficient and Kendall's τ, over time. The rolling window estimation is based on a window length of $m = 250$. Both measures develop in a similar manner. Nonetheless, there are some visible distinctions. Pearson's cor-

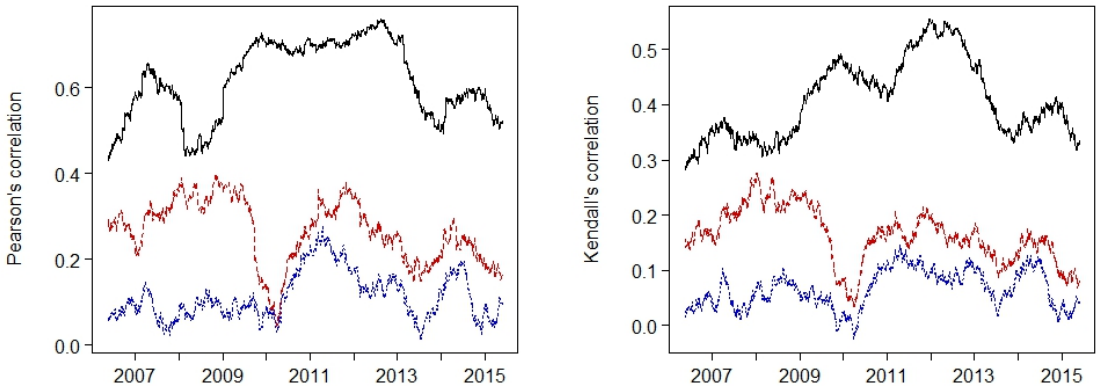

Figure 6: Rolling window estimation of Pearson's correlation coefficient and Kendall's τ for the residuals of DAX and DJ (black), DAX and Nikkei (red) and DJ and Nikkei (blue). The length of the rolling window is fixed at $m = 250$.

COPRollingcorr

relation coefficient is constantly positive over the considered time period for all couples of indices. Negative values of Kendall's τ appear solely for Dow Jones and Nikkei. Until 2009, the dependence between DAX and Nikkei is substantially higher than between Dow Jones and Nikkei. In the subsequent years, this difference is a lot smaller. It is also interesting to see that the correlation between DAX and Dow Jones increases considerably during the global financial crisis around 2009. This observation does not apply to the two remaining pairs of indices. Their correlation curves either drop or remain constant at that time. In view of the upcoming copula estimation, it is worth noticing that the dependence between the residuals of DAX and Dow Jones is by far the strongest over the entire time period. This finding leads to the presumption that the structure of the time-varying HAC does not change with time.

As in Härdle et al. (2010), the application of HAC-based distributions to investigate the dependencies between the residuals is motivated by estimating three parametric models via a rolling window approach. Likewise, these parametric models correspond to a three-dimensional HAC, a three-dimensional exchangeable Archimedean copula (AC), and a three-dimensional Gaussian copula. The HAC and the AC are based on Gumbel generators. The marginal distributions of the residuals are estimated nonparametrically. The models are assessed according to the Bayesian information criterion (BIC) which makes use of the maximum likelihood (ML) criterion and penalizes for the number of copula parameters denoted

by p. In line with Härdle et al. (2010), the BIC is calculated by $BIC = -2ML + 2\log(p)$. The changes of BIC for the three models are displayed in Figure 7. Whereas the BIC for the

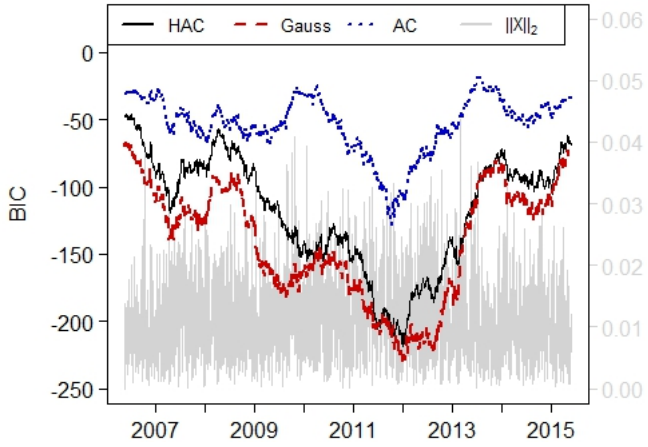

Figure 7: Rolling window estimation of BIC for multivariate distributions of the indices based on HAC, exchangeable Archimedean copula and Gauss copula. The window length is fixed at $m = 250$. The grey line depicts the time-varying L_2 norm of the difference in the parameter matrices of the HAC. The dots indicate that a change in the structure of the HAC occured.

COPRollingBIC

HAC and the Gaussian copula behave very similarly, the BIC for the AC is steadily inferior. The structure of the HAC is not subject to any changes since dots do not appear in the plot. It is equal to $s = ((\text{DAX DJ}) \text{ Nikkei})$ which has already been seen in Figure 6. The grey line in Figure 7 shows the changes of $||\hat{\Theta}_t - \hat{\Theta}_{t-1}||_2$. It is also present in Härdle et al. (2010). $\hat{\Theta}_t$ stands for the matrix of estimated dependence parameters of the HAC at time point t and $||\cdot||_2$ is the L_2 norm for a matrix. The definition corresponds to $||\mathrm{A}||_2 = \sqrt{\lambda_{\max}(\mathrm{A}^{\mathrm{T}}\mathrm{A})}$ where $\lambda_{\max}$ denotes the largest eigenvalue of matrix $\mathrm{A}^{\mathrm{T}}\mathrm{A}$. There are times when the variation of the dependence parameters is greater, and times when it is negligible. A revealing relationship between the BIC, the structure parameter and the variation of the dependence parameters is not visible. Figure 7 does not provide any help in detecting intervals which are characterized by homogeneous dependencies between the residuals. In summary, Figure 7 tells us that the HAC is preferable over the exchangeable AC when using BIC as a measure of the goodness-of-fit in a rolling window approach. The Gaussian copula exhibits a similarly good fit over time as the HAC. However, due to its inability to model tail dependence, it is not considered in the following analysis.

5.3 Local Parametric Estimation

In the two preceding sections, some interesting observations were made. The residuals do not follow a normal distribution which motivates nonparametric estimation of the marginal distributions for the HAC. Moreover, the use of HAC-based distributions seems to provide a good model fit. The time-varying nature of the dependencies between the residuals was clearly detectable. It is anticipated, however, that solely the strength in dependence parameters evolves across time, whereas the structure of the HAC is expected to remain unchanged. In this section, the sequential testing procedure described in Section 3 is applied to the residuals. Recall that it is carried out twice. The first run uses the pre-simulated critical values from Section 3.3.1, whereas the second run builds on the adaptively simulated critical values as explained in Section 3.3.2.

The setup for the sequential testing procedure corresponds to the one given in Section 3.2. The lengths of the interval candidates are determined via the formula $m_k = [m_0 c^k]$ where $m_0 = 40$, $c = 1.25$ and $k = 1, 2, ..., 10$. The metaparameters ρ and r are fixed at 0.5. Recall that in order to conduct the test of homogeneity on interval I_k, the next longer interval I_{k+1} has to be taken into account as illustrated in Figure 2. This means that the largest interval I_{11} potentially used during the run time of the procedure has a length of $m_{11} = 466$. Thus, the first 466 time points are exempt from the estimation. The first estimated HAC is obtained for $t = 467$. For the HAC, only Gumbel generators are considered. Before starting the procedure, the HAC is estimated once for the entire sample. The globally estimated HAC is given by $\hat{C}_1\{\hat{C}_2(\text{DAX}, \text{DJ}; 1.661), \text{Nikkei}; 1.15\}$.

5.3.1 Pre-simulated Critical Values

The estimation results of the sequential testing procedure based on the pre-simulated critical values are presented in Figure 8 in the same manner as in Härdle et al. (2010). The first plot depicts the time variation of the estimated structure parameter of the HAC. At four points in time, the structure amounts to $\hat{s} = ((1.3).2) = ((\text{DAX Nikkei}) \text{ DJ})$. This structure appears merely in the beginning of the estimation period. The initial variation of the structure parameter occurs at times when the two highest correlation curves from Figure 6 are relatively close. At all other times, the structure equals $\hat{s} = ((1.2).3) = ((\text{DAX DJ}) \text{ Nikkei})$ and thus corresponds to the presumption made from the rolling window estimation of the correlation coefficients. The second graph shows the evolution of the dependence parameters of the HAC

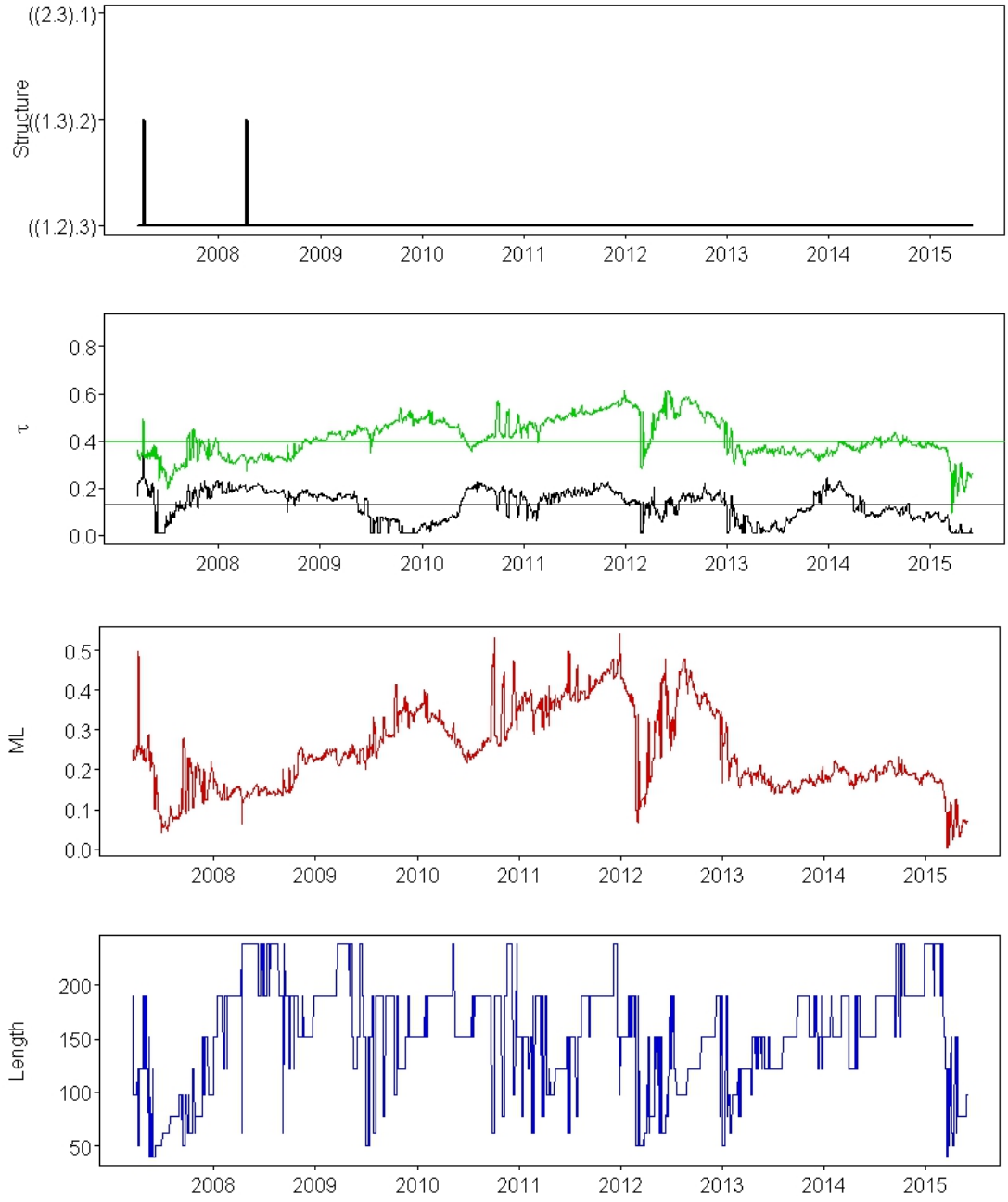

Figure 8: Time variation of copula parameters, maximum likelihood and interval lengths using pre-simulated critical values for DAX, DJ and Nikkei. The horizontal lines in the second plot correspond to the dependence parameters of the global HAC.

COPlcpgraphs

represented by τ_1 and τ_2. The green line corresponds to the larger dependence parameter τ_1, whereas the black line stands for the smaller dependence parameter τ_2. The two horizontal lines in the graph represent the globally estimated dependence parameters from above. In

the initial period, the two time-varying parameters develop similarly. However, they move away from each other and become more distant from the middle of 2008. In the subsequent years, they repeatedly approach each other and drift away again. Moreover, the time-varying dependence parameters move around the global dependence parameters, but show substantial deviations. In the period from 2013 until 2015, the larger dependence parameter remains relatively constant at the estimated value of the global HAC. It can be seen clearly, that the sequential testing procedure even accounts for relatively slight changes in the dependence parameters. What is also remarkable here is the fact that the first change in the structure parameter goes in line with a sudden jump upwards by both dependence parameters. The dynamics of the ML criteria obtained on the homogeneous intervals are depicted in the third graph. The ML values are corrected for the lengths of the corresponding intervals of homogeneity. In this manner, they represent the expected log-likelihood of a single observation within the respective homogeneous interval. The ML criterion is used here as the goodness-of-fit measure. Roughly speaking, the fit of the HAC improves until 2012/2013 and declines thereafter. The first change in the structure, which comes along with a jump in the dependence parameters, is also visible in the dynamics of the fit of the HAC. The ML criterion shoots upwards at that time. Such sharp changes also occur for instance around 2011 and 2012. In summary, the fit of the HAC evolves in a similar manner as the larger dependence parameter τ_1. The bottom picture illustrates the changes in the length of the intervals of homogeneity. Before 2008, a relatively large drop in the fit and the dependence parameters appears jointly with a drop in the length of the interval. Thereafter, the length of the homogeneous intervals grows. During times that are shaped by a slightly higher variation in the dependence parameters as for example around 2011 or 2012, the intervals of homogeneity are shorter. While the variation in the greater parameter levels out from 2013 until 2015, the length of the intervals slowly increases. In 2015, there is another substantial reduction in the interval length coming along with a sudden decline in the curves of the parameters and the ML criterion.

This application of the sequential testing procedure relies on the critical values that were simulated beforehand according to some fixed parameter constellations set by the researcher. The respective critical values are chosen such that the underlying parameter constellations are closest to the estimated parameters obtained on the relevant interval. Figure 9 shows how often the different parameter constellations are picked throughout the procedure. It can be seen that most of the obtained parameter estimates lie closest to the parameter constellations

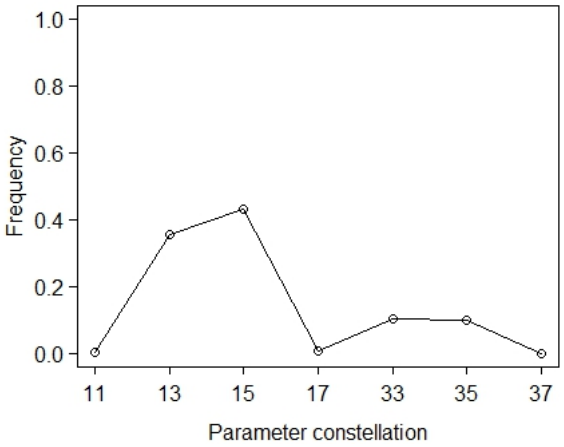

Figure 9: Distribution of the selected parameter constellations. The label 11 on the x-axis stands for the constellation $(\tau_1, \tau_2) = (0.1, 0.1)$, the label 13 represents $(\tau_1, \tau_2) = (0.3, 0.1)$ and so on.

$\{\tau_1, \tau_2\} \in \{0.1, 0.3, 0.5\}^2$, where $\tau_1 > \tau_2$ and $\tau_2 = 0.1$. The other parameter constellations are chosen in many fewer cases. Some of them seldom, and some never. These facts demonstrate that setting parameter constellations in advance without having a look at the data can be inefficient. Figure 10 enables a look at the data at hand. It presents the estimated parameter constellations obtained for every point in time and interval candidate. The red points in the plot denote the parameter constellations set by the researcher in advance. It can be observed

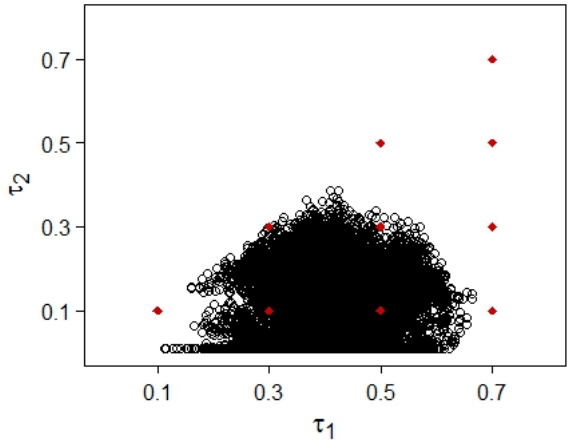

Figure 10: Scatterplot of estimated parameter constellations for every point in time and interval candidate. The red points mark the parameter constellations fixed by the researcher beforehand.

that the estimated parameter constellations are concentrated at the bottom center of the plot window. Some of the red points lie in the cloud of black points, whereas others are located far away from it. These findings explain why the parameter constellations $\{\tau_1, \tau_2\} \in \{0.5, 0.7\}^2$ with $\tau_1 \geq \tau_2$ are never chosen. Moreover, the choice of the closest parameter constellations gives rise to inaccuracies since the critical values vary with the underlying parameters. This fact was observed in Figure 3. Figure 10 reveals that the pre-set parameter constellations could be chosen such that the area where the estimated parameter constellations lie is split more subtle. In this way, the inaccuracies could be reduced. Since the goal of the present study is to dispel the inaccuracies, the subsequent section concerns the estimation results of the sequential testing procedure deploying the second approach to simulating the critical values. The second approach does not choose the closest parameter constellations, but directly simulates the critical values on the basis of the estimated parameters on the relevant interval. Thus, these critical values are considered as the exact critical values.

5.3.2 Adaptively Simulated Critical Values

The estimation results of the sequential testing procedure based on adaptively simulated critical values are illustrated in Figure 11. Considering the top graph, one notices that the structure shifts several times in the initial period. In six cases, the structure amounts to $\hat{s} = ((1.3).2) = ((\text{DAX Nikkei}) \text{ DJ})$. In all other cases, the structure is robust at $\hat{s} = ((1.2).3) = ((\text{DAX DJ}) \text{ Nikkei})$ and corresponds to the structure suspected earlier. The second graph provides the dynamics of the dependence parameters of the HAC denoted by τ_1 and τ_2 as before. In the beginning of the time period, the two dependence parameters exhibit a relatively small distance between each other. However, this distance starts growing around the middle of 2008. Thereafter, the dynamic behaviour of the parameters is shaped by mutual approaches as well as drifts away from each other. In addition, both dependence parameters wander around their global equivalent. From 2013 to 2015, the greater dependence parameter does not show big deviations from the respective global dependence parameter. The changes in the structure to $\hat{s} = ((\text{DAX Nikkei}) \text{ DJ})$ can be seen in the plot of the parameters as well. Both parameters leap up simultaneously. At the same time, the ML criteria exhibit the highest values of the whole estimation period. After this, the fit of the HAC decreases rather abruptly and rises again until about 2012. Then, it drops tremendously and grows anew featuring an increased variance. The period from 2013 until 2015 is characterized by a stable fit of the HAC. The dynamic behaviour of the fit resembles the one of the larger dependence

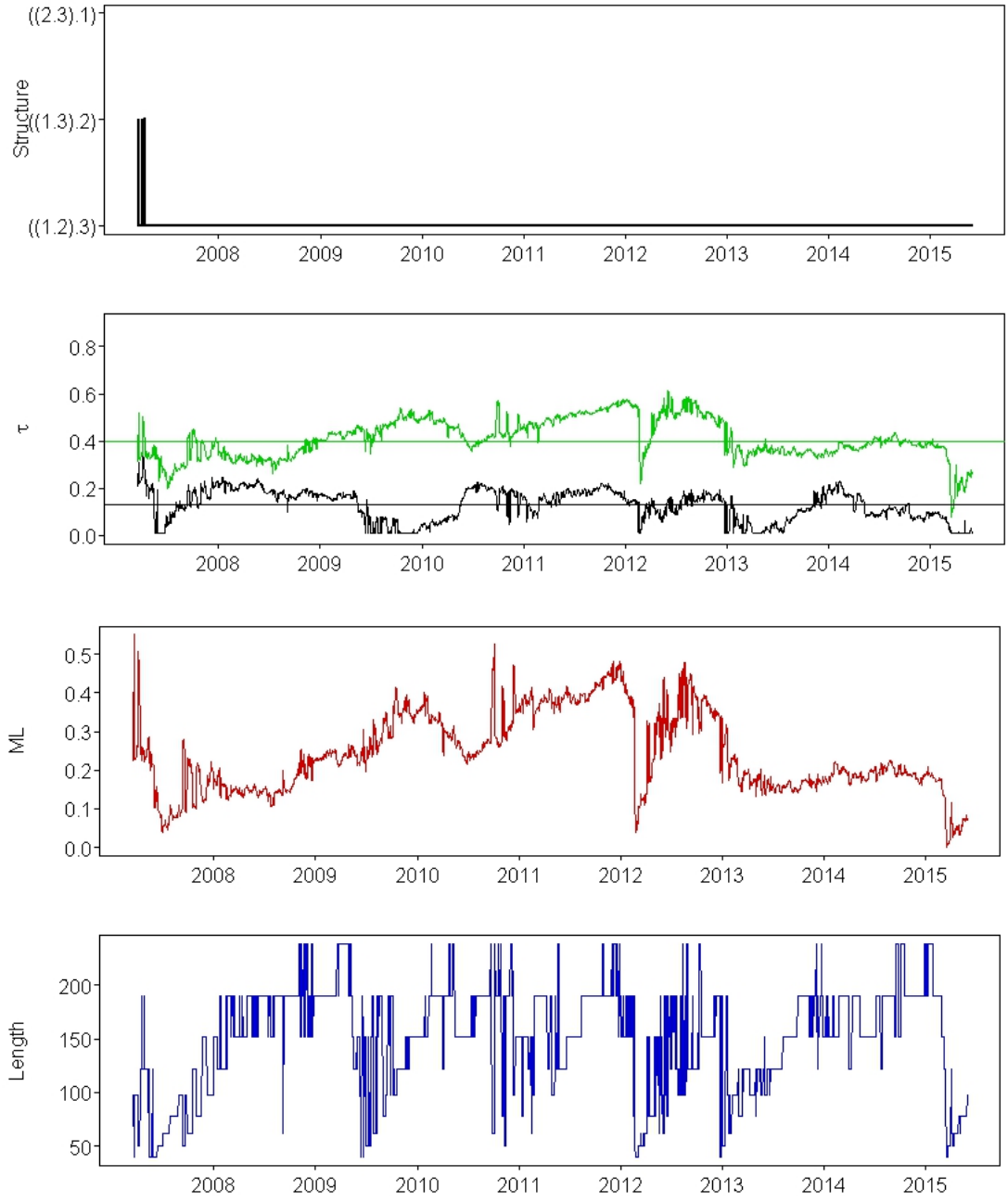

Figure 11: Time variation of copula parameters, maximum likelihood and interval length using adaptively simulated critical values for DAX, DJ and Nikkei. The horizontal lines in the second plot correspond to the dependence parameters of the global HAC.

COPlcpgraphs

parameter. The length of the homogeneous intervals are depicted in the bottom plot. While the intervals are rather short in the initial period, they get longer until the middle of 2009. In general, the curve of the length is characterized by several ups and downs. However, it

is striking that larger drops tend to occur at times when the dependence parameters also exhibit larger changes. It is clearly visible, for example, that the sharp reduction of the interval length in the beginning of 2012 is accompanied by a substantial fall of the greater dependence parameter. Thereafter, the larger dependence parameter remains quite stable and the homogeneous intervals grow over about two years. Only in 2015, the length of the intervals falls back to $m_0 = 40$ when the parameters decrease as well. Especially the larger dependence parameter shows a sharp drop.

The foregoing and the present section provide the two estimation results of the sequential testing procedure. Both approaches differ in the choice of the critical values for the statistical tests. Whereas some deviations of the two estimation results are already noticeable from the previous graphs, the next section intends to give a deeper insight into the distinctions.

5.3.3 Comparison

The two applications of the sequential testing procedure provide different results in cases where the intervals of homogeneity are not identical. Identical intervals are chosen in 73.75 per cent of all estimation points. The following table contains the number of different test decisions per step. In addition, it comprises the number of tests carried out per step by both approaches. The number of different test decisions is relatively low at the first test levels of the sequential testing procedure. However, it increases steadily until it reaches its maximum at level $k = 7$. Thereafter, it declines and equals zero for $k = 9, 10$. Since the number of tests per step that are conducted by both approaches reduces with higher k, the increase in the percentage of different test decisions is reinforced.

k	1	2	3	4	5	6	7	8
no. of different test decisions	25	28	35	39	75	100	151	109
no. of tests conducted per step	2141	2097	2021	1916	1787	1615	1332	774

Table 2: Distribution of different test decisions over the levels of the test steps. The second row contains the number of tests conducted per step by both approaches.

Different test decisions imply that the two approaches choose distinct intervals of homogeneity for the estimation. Hence, the comparison of the two estimation results next considers the differences in the length of the selected intervals of homogeneity. The upper plot of Figure

12 shows the differences in the number of test steps used per point in time. Positive values indicate that the pre-simulation approach makes use of more test steps to detect the homogeneous interval. The selected interval is greater accordingly. Negative values mean that the approach with adaptively simulated critical values carries out more tests and thus chooses the longer interval. Considering the difference in the number of test steps can be compared to an analysis of the difference in interval lengths in per cent. Due to the evolution of the intervals via a geometric grid, the absolute prolongation from one interval to the next larger one increases with the level of the test step. However, the prolongation is constant over all single test steps when measured in per cent. In fact, there are slight deviations from this

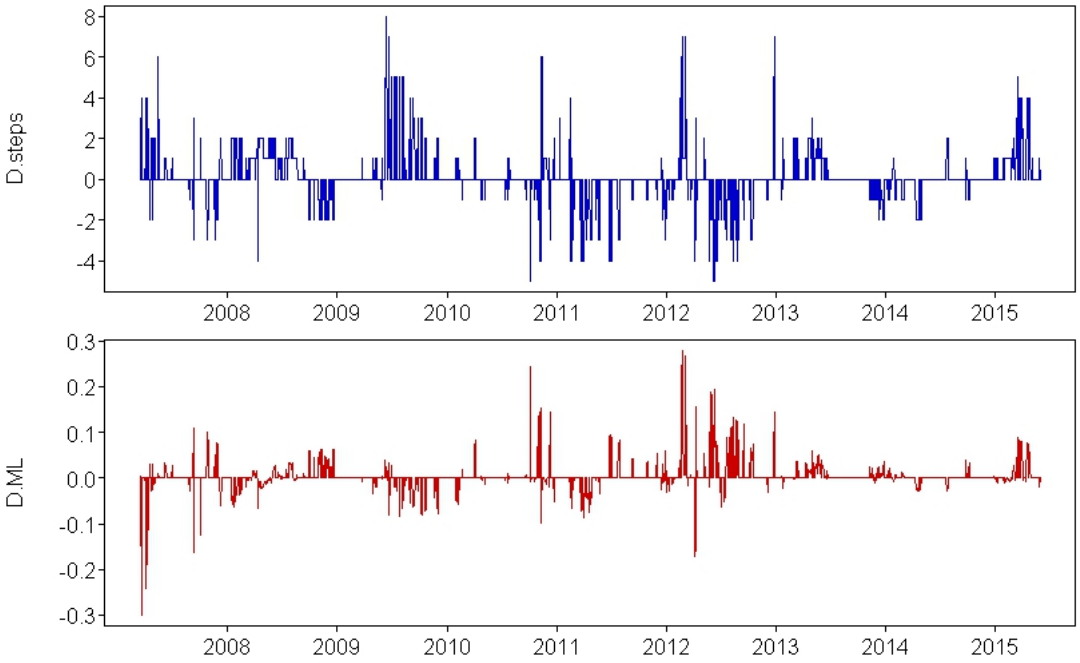

Figure 12: Time variation of the difference in the number of test steps and maximum likelihood for the two approaches to simulating the critical values. In the upper plot, positive values mean that the pre-simulation approach conducts more test steps per point in time than the second approach. Negative values declare the opposite. In the maximum likelihood plot, positive values indicate a higher goodness-of-fit for the pre-simulation approach, whereas the opposite holds for negative values.

COPlcpdiffMLI

constant percentage since the interval lengths are rounded to the next smaller integer. This is neglected here. If the difference in the number of test steps amounts to k, the interval of homogeneity is by $(1.25^k \times 100 - 100)$ per cent greater for the less restrictive approach

no matter at which test step the different test decision occurs. The plot demonstrates that there are substantial distinctions. Furthermore, it is remarkable that longer intervals for one approach tend to appear in clusters. There are times when the pre-simulation approach tends to choose longer intervals, for instance between 2009 and 2010. The algorithm based on the adaptive simulation approach stops several test steps before. Greater intervals are selected by this approach particularly from 2011 to 2013. The pre-simulation approach leads to a rejection of the null hypothesis some test steps in advance. From 2013 until 2015, the homogeneous intervals do not differ much in length on a percentage basis. In summary, one can say that the differences in interval length do not arise only by small differences in the number of conducted test steps, but also by larger differences. In particular, the approach based on pre-simulated critical values tests six to eight times more per point in time on some few occasions. There is a minor tendency that for the given data this approach selects larger intervals of homogeneity than the adaptive simulation approach. In order to assess these differences, have a look at the bottom plot of Figure 12. It presents the differences in the ML criterion. The pre-simulation approach is superior when the difference is positive and inferior in the opposite case. A first glance at the plot reveals that the pre-simulation approach is superior in more cases. However, there are times when the adaptive simulation approach almost steadily provides a better fit as for example between 2009 and 2010. At the same time, it is more restrictive in that it picks shorter intervals of homogeneity. During the time from 2011 to 2013, the goodness-of-fit is mostly better for the pre-simulation approach. This period is featured by higher differences in the fit and larger intervals of homogeneity for the adaptive simulation approach. Recalling Figure 8 and 11, it can be observed that the estimated dependence parameters are noisy at that time. The remaining time period does not show big deviations in the ML criteria. Finally, it has to be pointed out that the adaptive simulation approach, which is conceived to provide more precise results, is not globally superior regarding the model fit measured by the ML criterion. Besides, when assessing model fit, one should take into account that simulating the critical values adaptively demands way more calculation effort than simulating from solely ten different parameter constellations. This fact can be interpreted as higher costs for the adaptive simulation approach which are not reflected in the ML criterion. In addition, it is important to bear in mind that the ML criterion does not provide information about the significance of the distinctions in the fit of the two approaches. Above all, it does not indicate whether the model with the better fit is the true one.

Figure 13 provides information about the absolute length of the selected intervals of homogeneity for both approaches. The labels on the x-axis denote the number of observations within one interval. The results of the pre-simulation approach are represented by the black line, and the results of the second approach by the red line. The distribution of the interval length looks very similar for both approaches. More conspicuous distinctions can be spotted for the two greatest interval lengths. The pre-simulation approach chooses the interval length $|I| = 190$ more seldom than the second approach, but allows for $|I| = 238$ more often. Note that the largest possible interval of homogeneity is never chosen. If the procedure reaches the test step $k = 9$, the null hypothesis of parameter homogeneity is definitely rejected. The interval lengths that are chosen most frequently are $|I| = 152$ and $|I| = 190$. The other interval lengths are far more rarely selected. All in all, this plot demonstrates that the length of the homogeneous intervals varies. It might be suboptimal to set a constant interval length such as $m = 250$ in the classical rolling window approach before carrying out the estimation. If the analysis of the present study was to come up with a rule of thumb for the interval length, the suggestion would be $|I| = 190$. Indeed, such a suggestion should be treated with caution since the applied procedure makes use of metaparameters that are set by the researcher beforehand and influence the outcomes. Examples of such metaparameters are the level of risk given by $r = 0.5$ or the parameter $\rho = 0.5$ which can both be interpreted as counterparts of the ordinary significance level (Čížek et al., 2009).

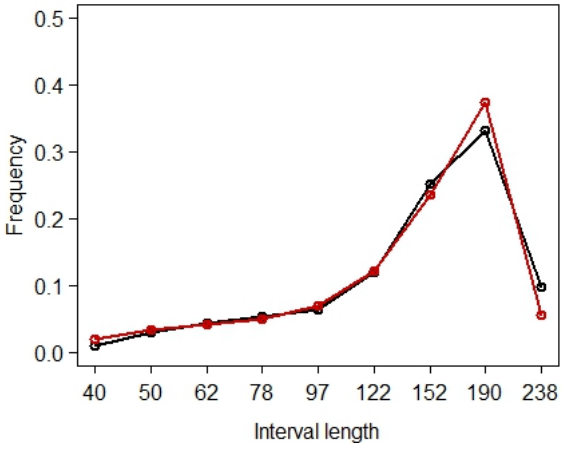

Figure 13: Distribution of the length of the selected intervals of homogeneity. The black line represents the pre-simulation approach, whereas the red line stands for the adaptive simulation approach.

The second approach was introduced in order to wipe out the inaccuracies induced by the pre-simulation approach. The input that makes the difference is the critical values which are simulated adaptively during the run of the sequential testing procedure. Figure 14 shows how the adaptively simulated critical values are distributed around the corresponding critical value taken from the pre-simulations. This analysis is restricted to the single test steps that are carried out in both runs. If one approach uses more test steps than the other at one point

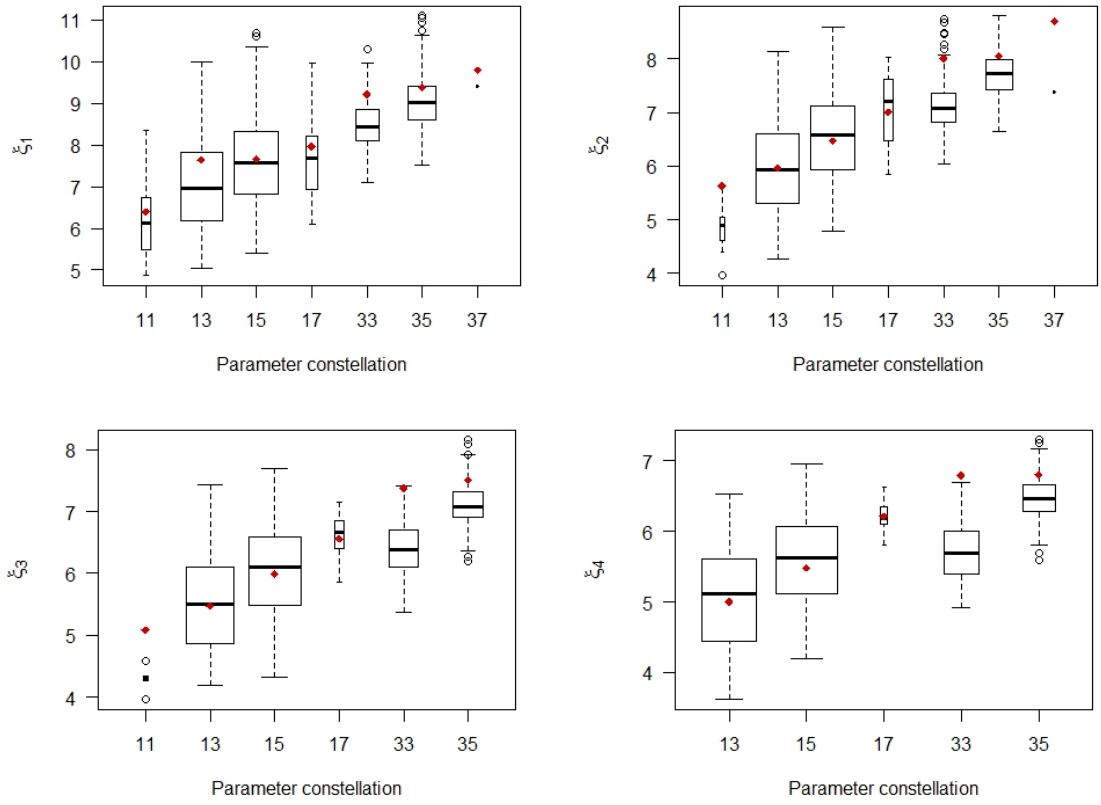

Figure 14: Distribution of the adaptively simulated critical values around the respective pre-simulated critical value. The label 11 on the x-axis stands for the constellation $(\tau_1, \tau_2) = (0.1, 0.1)$, the label 13 represents $(\tau_1, \tau_2) = (0.3, 0.1)$ and so on. The red points mark the pre-simulated critical value for the corresponding parameter constellation. The width of the boxes is proportional to the square root of the number of adaptively simulated critical values per group. The four plots depict the results for the first four test steps, $k = 1, ..., 4$.

COPlcpcompcv

in time, the associated critical values are ignored. The labels on the x-axis stand for the parameter constellation. For instance, the label 11 refers to $(\tau_1, \tau_2) = (0.1, 0.1)$ and the label 13 to $(\tau_1, \tau_2) = (0.3, 0.1)$. The red points indicate the pre-simulated critical value for the

respective parameter constellation. The width of the boxes is proportional to the square root of the number of critical values belonging to one group. The four plots refer to the results from the first four test steps, $k = 1, .., 4$. The results for the test steps $k = 5, ..., 8$ can be found in the appendix. Test step $k = 9$ is not shown since all pre-simulated and adaptively simulated critical values equal zero. In general, the plots demonstrate that higher values of (τ_1, τ_2) tend to result in higher critical values. Additionally, it can be observed that a higher k leads to smaller critical values. The parameter pairs most frequently chosen are $(\tau_1, \tau_2) \in \{0.1, 0.3, 0.5\}^2$, where $\tau_1 > \tau_2$ and $\tau_2 = 0.1$. The adaptively simulated critical values are relatively symmetric around the critical value obtained from these parameter constellations. However, the deviations are substantial. Looking at the lengths of the boxplots for the labels 13 and 15, one notices that the adaptive critical values are spread over approximately three integer values or more. For the parameter pairs $(\tau_1, \tau_2) = \{0.3, 0.5\}^2$ with $\tau_1 \geq \tau_2$, the pre-simulated critical value is rather located at the top end of the distribution of the adaptively simulated critical values. Such a case indicates that whenever these parameter constellations are chosen to be the closest ones, the second approach tends to be more restrictive in the tests than the pre-simulation approach. To sum up, Figure 14 clearly shows that the adaptively simulated critical values can cause essential differences in the single test decisions. In order to break down these deviations into a single number, consider Table 3. It contains the average absolute deviation of the adaptively simulated critical values from the pre-simulated critical

	11	13	15	17	33	35	37
ξ_1	0.824	0.989	0.821	0.678	0.805	0.593	0.380
ξ_2	0.793	0.677	0.645	0.547	0.916	0.443	1.310
ξ_3	0.788	0.631	0.570	0.309	1.110	0.351	NA
ξ_4	NA	0.589	0.517	0.169	1.096	0.364	NA
ξ_5	NA	0.527	0.523	NA	1.133	0.377	NA
ξ_6	NA	0.452	0.439	NA	1.489	0.362	NA
ξ_7	NA	0.377	0.378	NA	2.304	0.351	NA
ξ_8	NA	1.188	0.680	NA	2.520	1.660	NA

Table 3: Average absolute deviation of the adaptively simulated critical values from the pre-simulated critical value of the respective parameter constellation for test steps $k = 1, ..., 8$. Averages that are marked grey are computed from less than 30 critical values.

value of the respective parameter constellation for the first eight test steps. The grey marked numbers indicate that these averages are computed from less than 30 critical values. The label NA states that the respective parameter constellation is not selected in the pre-simulation approach or corresponding adaptively simulated critical values are not available. The averages show that the deviations are not negligible. In most of the cases, the average deviation amounts to a value greater than 0.5. For the parameter constellation 33, the averages take on values that are even greater than 2. For some parameter constellations, the average absolute deviation from the pre-simulated critical value almost steadily decreases with the test step. However, there are a few notable exceptions. Note that these numbers do not indicate whether one approach tends to be more restrictive than the other for a certain parameter constellation.

This section intended to give a deeper insight into the differences of the estimation results of the two diverse approaches to simulating the critical values. At first, the distinctions in the number of conducted test steps were examined. It was found that the two approaches alternate in being more restrictive in the tests. This finding is easy to explain since the choice of the closest parameter constellation requires that the estimated parameters are rounded either up or down. Accordingly, the selected pre-simulated critical value is greater or smaller than the adaptively simulated one. The differences in the interval length arise from just a few more as well as from up to eight more test steps per point in time for one approach. The analysis of the differences in the ML criteria showed that neither of the two approaches is continuously superior. In a next step, the distributions of the absolute length of the intervals of homogeneity were studied. It was seen that the length of the intervals varies. Beyond that, the most selected interval length is the same for both approaches and amounts to $|I| = 190$. Furthermore, the source that causes the differences in the results, namely the critical values, was regarded more thoroughly. The deviations of the adaptively simulated critical values from the respective pre-simulated critical values are substantial and should not be ignored per se.

6 Conclusions

The present empirical study aims at analysing the time-varying nature of financial contagion between international stock markets. In order to do so, a time-varying HAC model with Gumbel generators is fitted to daily log returns of DAX, Dow Jones and Nikkei. A time-varying

HAC model enables to account not only for a change in the strength of the dependence parameters, but also for a change in the order of the variables. The time-dependent copula parameters are obtained by means of the local parametric approach introduced in Spokoiny (1998). At each point of the considered time period, the largest possible interval of homogeneity is selected via a sequential testing procedure and then used for the estimation of the HAC. The local parametric approach is applied to the data twice. The two runs differ in the choice of the critical values that are used for the single test steps of the procedure. The first run makes use of critical values that were simulated on the basis of some pre-defined parameter constellations and thus corresponds to the approach employed in Härdle et al. (2010). The second run intends to provide a refinement of the estimation results of the first run by adaptively simulating the critical values according to the "true" underlying parameters represented by the estimates obtained on the considered interval. Finally, both estimation results are compared.

The application of the local parametric approach to real world data leads to several interesting observations. First of all, it was seen that the approach accounts not only for jumps in the dependence parameters, but also for relatively small changes. The estimated dependence parameters of the HAC exhibit substantial variation over time. Moreover, the approach detects several shifts in the structure parameter of the HAC. It can be thus concluded that changes in the distribution occur and should not be neglected, for instance, by applying exchangeable Archimedean copulas. Second of all, the length of the selected intervals of homogeneity varies from 40 to 238 observations. Shorter intervals are selected at times when the variation in the parameters is higher. The length of the homogeneous intervals tends to grow when the variation in the parameters is less intense. The most-selected interval length of 190 observations could be regarded as a rule of thumb for daily log returns. Nonetheless, the results point to the fact that a rolling window estimation with a fixed window length can be suboptimal in the sense that it is too rigid to detect the "true" transitions in parameters. Third of all, the second run of the sequential testing procedure which makes use of adaptively simulated critical values provides different intervals of homogeneity in more than 25 per cent of all estimation points. This approach aims at refining the method based on pre-simulated critical values. The pre-simulation approach disregards the impact of the underlying true parameters on the critical values to some extent and therefore causes inaccuracies. The analysis of the estimation results reveals that there are substantial deviations of the adaptively simulated critical values from the corresponding pre-simulated critical value. These findings indicate

that it cannot be optimal to discount these inaccuracies per se.

Although the adaptive simulation of the critical values intends to improve the approach which builds on the pre-simulations, it also entails some disadvantages. Since it enforces the simulation of the critical value for each point in time and each considered interval separately, it is extremely more time demanding to run the sequential testing procedure. In the present empirical study, a HAC model is estimated at 2141 points in time. Under the assumption of homogeneity this would demand the simulation of 2141×10 critical values. By contrast, the pre-simulation approach requires solely the simulation of 100 critical values. Besides, the adaptively simulated critical values are obtained from a number of samples restricted to $N = 1,000$, whereas the pre-simulated critical values originate from $N = 10,000$ samples. A greater number of samples results in a better degree of precision for the critical values. To combat this, the critical values are calculated to two decimal places by both approaches. However, it is likely that even this restriction is insufficient to generate accurate critical values. In Cuddington and Navidi (2011), it is pointed out that in practice the number of replications does oftentimes not suffice to ensure the desired degree of precision for the critical values. In addition, recommendations for approximating the number of replications necessary for a given degree of accuracy are made. These recommendations are not easily transferable to the present study since they involve the significance level of the test. In the applied sequential choice of the critical values, however, the significance level is not clearly defined, but represented by two metaparameters ρ and r. Recall, that the two parameters can be interpreted as counterparts of the ordinary significance level.

Alternative ways to get the critical values can be found in Härdle et al. (2012) and Neubauer (2012). In Härdle et al. (2012), the critical values are simulated for reasonable parameter constellations. They are inferred from parameter values which the authors have obtained from previous estimates on the basis of the data at hand. In this manner, the critical values are simulated in a more data-driven way than in Härdle et al. (2010), but do not demand as much calculation time as the adaptive simulation approach from the present study. In Neubauer (2012), a completely different method to calculate the critical values is introduced. This research work concerns time-varying R-vine copula models. In order to avoid the extensive computation time, the critical values are approximated linearly. This approximation of the critical values depends on Kendall's τ, the metaparameter ρ, the number of observations within the relevant interval and the maximum number of test steps. Although inducing inac-

curacies of the critical values, this method serves as an interesting alternative to the approach based on adaptively simulated critical values.

References

Andreou, E. and Ghysels, E. (2008). Structural breaks in financial time series. In Andersen, T. G., Davis, R. A., Kreiss, J. P., and Mikosch, T. (eds), *Handbook of Financial Time Series*, Springer, New York.

Bergmann, D. R., Securato, J. R., Ferreira Savoia, J. R., and do Rosário Contani, E. A. (2015). U.S. subprime financial crisis contagion on BRIC and European Union stock markets, *Revista de Administração (São Paulo)*, 50(2): 229–240.

Bollerslev, T. (1986). Generalized autoregressive conditional heteroskedasticity, *Journal of Econometrics*, 31(3): 307–327.

Cont, R. (2005). Volatility clustering in financial markets: Empirical facts and agent-based models. In Kirman, A. and Teyssiere, G. (eds), *Long memory in economics*, Springer.

Cuddington, J. T. and Navidi, W. (2011). A critical assessment of simulated critical values, *Communications in Statistics – Simulation and Computation*, 40(5): 719–727.

Embrechts, P., Lindskog, F., and McNeil, A. (2001). Modelling dependence with copulas and applications to risk management, Preprint, ETH Zürich.

Genest, C. and MacKay, R. (1986). The joy of copulas: Bivariate distributions with uniform marginals, *The American Statistician*, 40(4): 280–283.

Giacomini, E., Härdle, W. K., and Spokoiny, V. (2006). Inhomogeneous dependency modelling with time varying copulae, Discussion Paper 075, SFB 649, Economic Risk.

Górecki, J. and Holeňa, M. (2013). Structure determination and estimation of hierarchical Archimedean copulas based on Kendall correlation matrix. In Appice, A., Ceci, M., Loglisci, C., Manco, G., Masciari, E., and Ras, Z. (eds), *New Frontiers in Mining Complex Patterns*, pp. 132–147, Springer, Heidelberg.

Härdle, W. K., Hautsch, N., and Mihoci, A. (2012). Local adaptive multiplicative error models for high-frequency forecasts, Discussion Paper 031, SFB 649, Economic Risk.

Härdle, W. K., Okhrin, O., and Okhrin, Y. (2010). Time varying hierarchical Archimedean copulae, Discussion Paper 018, SFB 649, Economic Risk.

Hoeffding, W. (1940). Massstabinvariante Korrelationstheorie, *Schriften des mathematischen Seminars und des Instituts für angewandte Mathematik der Universität Berlin*, 5: 181–233.

Hofert, M. and Maechler, M. (2011). Nested Archimedean copulas meet R: The nacopula package, *Journal of Statistical Software*, 39(9): 1–20.

Joe, H. (1997). *Multivariate Models and Dependence Concepts*. Chapman & Hall, London.

Kimberling, C. (1974). A probabilistic interpretation of complete monotonicity, *Aequationes Mathematicae*, 10(4): 152–164.

Mandelbrot, B. (1963). The variation of certain speculative prices, *The Journal of Business*, 36(4): 394–419.

McNeil, A. J. (2008). Sampling nested Archimedean copulas, *Journal Statistical Computation and Simulation*, 78(6): 567–581.

Mercurio, D. and Spokoiny, V. (2004). Statistical inference for time-inhomogeneous volatility models, *Annals of Statistics*, 32(2): 577–602.

Nelsen, R. (1999). *An Introduction to Copulas*. Springer, New York.

Neubauer, X. (2012). Local change point detection in time-varying R-vine copula models, Diploma thesis, Technische Universität München.

Okhrin, O., Okhrin, Y., and Schmid, W. (2013). On the structure and estimation of hierarchical Archimedean copulas, *Journal of Econometrics*, 173(2): 189–204.

Okhrin, O. and Ristig, A. (2014). Hierarchical Archimedean copulae: The HAC package, *Journal of Statistical Software*, 58(4): 224–234.

Patton, A. J. (2006). Modelling asymmetric exchange rate dependence, *International Economic Review*, 47(2): 527–556.

Rachev, S. T., Menn, C., and Fabozzi, F. J. (2005). *Fat-Tailed and Skewed Asset Return Distributions*. John Wiley & Sons, Inc., Hoboken, New Jersey.

Rodriguez, J. C. (2007). Measuring financial contagion: A copula approach, *Journal of Empirical Finance*, 14(3): 401–423.

Sklar, A. (1959). Fonctions de répartition à n dimensions et leures marges, *Publications de l'Institut de Statistique de l'Université de Paris*, 8: 229–231.

Spokoiny, V. (1998). Estimation of a function with discontinuities via local polynomial fit with an adaptive window choice, *The Annals of Statistics*, 26(4): 1356–1378.

Spokoiny, V. (2009). Multiscale local change point detection with applications to value-at-risk, *The Annals of Statistics*, 37(3): 1405–1436.

Čížek, P., Härdle, W. K., and Spokoiny, V. (2009). Adaptive pointwise estimation in time-inhomogeneous conditional heteroscedasticity models, *Econometrics Journal*, 12(2): 248–271.

A Figures

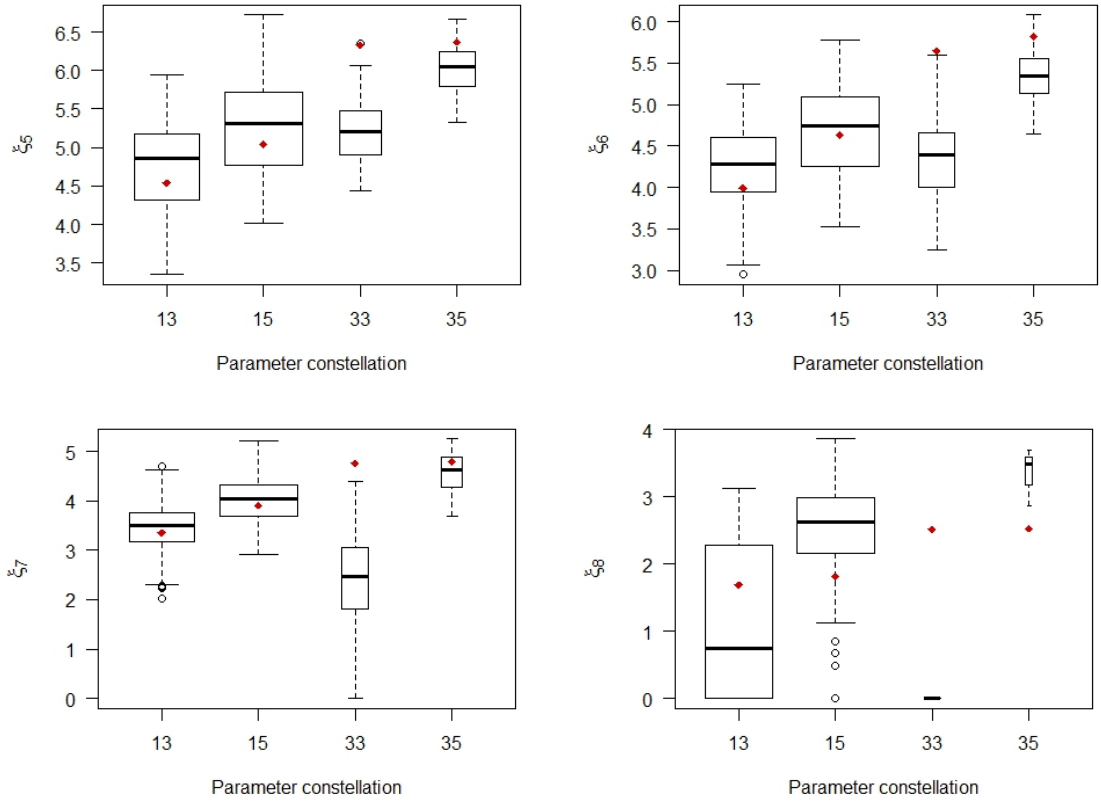

Figure 15: Distribution of the adaptively simulated critical values around the respective pre-simulated critical value. The label 11 on the x-axis stands for the constellation $(\tau_1, \tau_2) = (0.1, 0.1)$, the label 13 represents $(\tau_1, \tau_2) = (0.3, 0.1)$ and so on. The red points mark the pre-simulated critical value for the corresponding parameter constellation. The width of the boxes is proportional to the square root of the number of adaptively simulated critical values per group. The four plots depict the results for the test steps $k = 5, ..., 8$.

Declaration of Authorship

I hereby confirm that I have authored this Master thesis independently and without use of others than the indicated sources. All passages which are literally or in general matter taken out of publications or other sources are marked as such.

Berlin, December 09, 2015

Ramona Theresa Steck